

Conformations of 2,4-Diphenylpentane: A Quantum Chemistry and Gas-Phase Molecular Dynamics Simulation Study

Grant D. Smith* and Chakravarthy Ayyagari

Department of Materials Science and Engineering and Department of Chemical and Fuels Engineering, University of Utah, Salt Lake City, Utah 84112

Richard L. Jaffe

NASA Ames Research Center, Moffett Field, California 94035

Matthew Pekny† and Aaron Bernarbo

Department of Chemical Engineering, University of Missouri—Columbia, Columbia, Missouri 65211

Received: January 27, 1998; In Final Form: April 3, 1998

We report on the relative conformer energies and rotational energy barriers for meso and racemic 2,4-diphenylpentane (DPP) from ab initio electronic structure calculations. It is found that dispersion interactions between phenyl rings strongly influence the conformational geometries, necessitating the inclusion of electron correlation in both geometry optimizations and energy calculations. Furthermore, basis set superposition contributions to the phenyl–phenyl interactions, estimated by extracting the phenyl rings from the optimized DPP geometries and computing the basis set superposition error for the resulting benzene dimer configurations, are significant. An atomistic molecular mechanics force field is parametrized to reproduce our best values for the conformational energies and rotational energy barriers in DPP obtained from ab initio calculations. Conformational energy contour maps are presented for the DPP enantiomers, and their salient features are discussed. Gas-phase molecular dynamics simulations of DPP have been performed using the quantum chemistry based force field. Important entropic contributions to the conformer populations, due primarily to restricted phenyl group rotation, are discussed.

I. Introduction

While it is known that interactions between aromatic groups strongly influence the properties, including chain conformations, of polymers containing these groups, the nature of these effects is not well-understood. One of the most studied aromatic polymers is polystyrene. Recent molecular simulations of polystyrene^{1–8} reflect continued interest in the conformational properties and amorphous packing in this important polymer. Despite extensive experimental and modeling efforts, however, the conformational properties of polystyrene and the influence of aromatic interactions on both conformations and local structure are not fully understood. This is demonstrated by the limited success of molecular simulations using detailed atomistic models to reproduce experimentally measured X-ray and neutron structure factors (e.g., refs 1 and 2).

Much of our understanding of the conformational characteristics of polystyrene is based upon experimental studies of meso and racemic 2,4-diphenylpentane (DPP) and the enantiomers of the 2,4,6-triphenylheptane (TPH). These compounds can be considered polystyrene dimers and trimers, respectively. Far-infrared and depolarized Rayleigh scattering methods have been applied in the study of phenyl ring motion in these compounds,⁹ while conformational populations have been investigated by NMR vicinal coupling measurements,^{10–13} depolarized Rayleigh scattering (optical anisotropy),^{14,15} far-infrared and Raman

spectroscopy,¹⁶ ultrasonic relaxation measurements,^{17,18} and epimerization reactions.^{19,20} These compounds have also been the subject of both molecular mechanics^{21–23} and limited ab initio electronic structure calculations.²⁴ These studies seem to establish racemic *tt* (*r-tt*) as the lowest energy conformer of DPP. However, assignment of other low-energy conformers of racemic and meso DPP cannot be made unambiguously on the basis of these studies.

Molecular dynamics simulations of polystyrene oligomers, both as isolated molecules and in condensed phases (bulk liquid and solution), could greatly improve our understanding of the conformational properties of polystyrene, provided that the potential energy functions used in the simulations accurately describe both the conformational energetics and the influence of intermolecular interactions on conformations in condensed phases. Developing a validated conformational force field for polystyrene is challenging. Molecular mechanics and ab initio values for the conformer energies for isolated DPP molecules differ qualitatively from experimental estimates based upon liquid-phase measurements, indicative of strong condensed-phase effects. How these effects might be manifested is illustrated in Figure 1. Condensed-phase effects have been accounted for only approximately in molecular mechanics calculations through use of various schemes for screening intramolecular nonbonded interactions involving the phenyl rings.^{21–23} Additionally, while conformer populations based upon (condensed-phase) experimental data are available, only very limited data for rotational energy barriers,¹⁷ which to a

† Current address: Department of Chemical Engineering, University of Colorado, Boulder, CO 80309

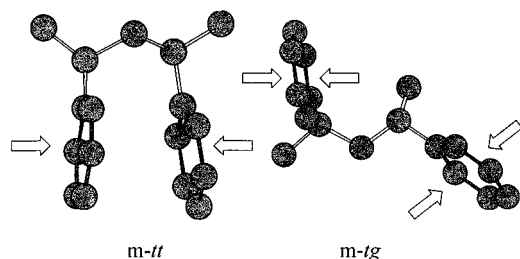


Figure 1. Optimized geometries (MP2/6-31G*) for the *m-tt* and *m-tg* conformers of 2,4-diphenylpentane. Hydrogen atoms are not shown. Arrows indicate faces of the phenyl rings available to interact with solvent. Phenyl–solvent interactions should stabilize the *m-tg* conformer relative to the *m-tt* conformer.

large extent determine polymer conformational dynamics, are available. Finally, *ab initio* calculations, which have been demonstrated to be a reliable source of conformational energetics for isolated molecules, have been performed previously for DPP only with a minimal basis set and without electron correlation. As demonstrated below, these data are insufficient to allow development of accurate potentials.

Our goal is to obtain a force field for polystyrene and its oligomers that will accurately describe the conformational energetics and condensed-phase interactions in these materials. In previous work, we presented a nonbonded force field for benzene based upon quantum chemistry studies of benzene dimer.²⁵ Molecular dynamics simulations of liquid benzene confirmed that this force field accurately reproduces interactions in the condensed phase.²⁵ We will employ this benzene force field and our alkane force field²⁶ to describe intramolecular nonbonded interactions in polystyrene and its oligomers, with the expectation that condensed-phase effects will also be accurately represented by these functions. In this paper we present results of an *ab initio* quantum chemistry study of the conformational characteristics of the polystyrene model molecules isopropylbenzene (IPB) and DPP. Using the nonbonded potential described above, we develop a molecular mechanics force field that accurately reproduces the conformational energetics of these model molecules. We have utilized a similar procedure in the parametrization of force fields for a number of polymers, including polyethylene,²⁶ poly(tetrafluoroethane),²⁷ poly(vinyl chloride),²⁸ poly(ethylene oxide),²⁹ and 1,4-polybutadiene.³⁰ We also discuss the conformational energy surfaces for the DPP enantiomers based upon molecular mechanics calculations and conformer populations in the gas phase from molecular dynamics simulations employing our quantum chemistry based force field. In upcoming papers, we will consider condensed-phase effects in DPP and TPH liquids and solutions, and the conformations and local structure of atactic polystyrene based upon molecular dynamics simulations.

II. Quantum Chemistry Calculations

The local conformational characteristics of polystyrene are determined by the energetics of rotations about the backbone dihedrals, the rotation of the phenyl rings, and the coupling of these rotations. To study the energetics of the phenyl ring rotation we consider IPB. To study the backbone torsions, and the intradyad coupling of these torsions, we consider the enantiomers DPP. Aspects of the quantum chemistry calculations on these compounds relevant to the force field parametrization are considered below. A more detailed discussion of the quantum chemistry can be found elsewhere.³¹

Previous Work. Previous quantum chemistry studies of IPB and DPP have been limited to SCF (incomplete basis set

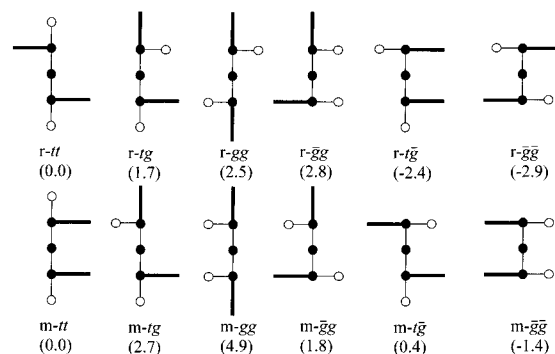


Figure 2. Schematic representation of the unique conformers of racemic and meso 2,4-diphenylpentane. Open circles represent methyl groups, closed methylene or methine groups, and dark lines phenyl groups. The numbers in parentheses are relative (to *r-tt* or *m-tt*) gas-phase entropies in J/mol·K.

Hartree–Fock) calculations using minimal basis sets, and limited calculations with a larger basis set for IPB only. Schaefer et al.³² examined the energetics of the phenyl ring rotation in IPB using SCF/STO-3G and limited SCF/6-31G geometry optimizations and energy calculations. Similar SCF/STO-3G calculations were performed by Lagowski and co-workers.³³ These studies found that the low-energy conformation of the phenyl ring corresponds to a torsional angle ψ of near 60° , with the phenyl ring eclipsing the methine hydrogen. The rotational energy barrier at $\psi = 150^\circ$ was found to depend on basis set (3.64 kcal/mol at the SCF/STO-3G level and 3.20 kcal/mol at the SCF/6-31G level). An *ab initio* study of *m*-DPP and *r*-DPP has been conducted by Lagowski and co-workers.²⁴ They determined the geometries and relative conformer energies of the six unique conformations of both enantiomers at the SCF/STO-3G level. These conformers are illustrated schematically in Figure 2. These results are discussed in the context of our calculations described below.

Level of Theory. The level of theory that must be employed in order to obtain accurate conformational geometries and energies from quantum chemistry calculations is dependent on the nature of the dominant interatomic nonbonded forces. If conformational geometries are determined primarily by either steric repulsion or electrostatic interactions, we have found that geometry optimization at the SCF level and subsequent energy calculations using correlated methods yield reasonably accurate conformational geometries and relative energies.^{26,29} If, however, dispersion effects are important in determining the geometry, SCF calculations are completely inadequate. This is clearly demonstrated for benzene dimer,³⁴ where we found that dispersion interactions between phenyl rings are more important than steric and electrostatic effects. In that case, SCF level geometry optimizations failed completely to yield the experimentally observed structure and binding energy of benzene dimer.

Interactions between phenyl rings strongly influence the local structure and conformations of polystyrene. Therefore, accurate quantum chemistry studies of polystyrene model molecules *must* include electron correlation in order to obtain reasonable representation of dispersion as well steric and electrostatic effects. Fortunately, Møller–Plesset (MP2) perturbation theory provides a good description of dispersion interactions in many cases. This is important in the case of DPP, because the large size of molecule precludes higher level treatments of electron correlation, especially in geometry optimizations. In particular, we found for benzene dimer that MP2/6-31G*/MP2/6-31G*

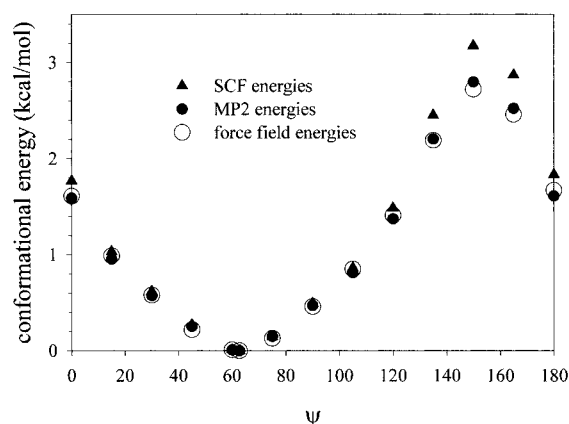


Figure 3. Conformational energy of isopropylbenzene as a function of the phenyl ring dihedral angle. Quantum chemistry values were obtained using a 6-31G* basis set at SCF/6-31G* geometries. Force field values are from the quantum chemistry based force field.

geometry/energy calculations, without basis set superposition error (BSSE) correction, gave complex geometries and binding energies in reasonable agreement with our best calculations. The latter calculations involved determining the dimer geometry at the MP2/6-311G(2d,2p) level with BSSE.³⁴ Subsequently, BSSE-corrected energies were determined at the MP2/6-311+G-(2df,2p) and MP4(SDTQ)/6-311G(2d,p) levels. For benzene dimer, the increased binding resulting from not correcting for BSSE approximately cancels the underestimation of dispersion effects due to basis set incompleteness at the 6-31G* level.

The geometries and energies of the most important conformers and rotational energy barriers in DPP were calculated at the MP2/6-31G*/MP2/6-31G* geometry/energy level. We also report results from SCF geometry optimizations with subsequent energy calculations at the MP2 level (SCF/D95*/MP2/D95*), and MP2 energy calculations using a larger basis set (MP2/6-31G*/MP2/6-311G**). To evaluate the phenyl–phenyl interactions for these geometries and thereby improve the estimates of the relative conformer energies in DPP, we extract the phenyl rings from the MP2/6-31G*-optimized geometries and treat them as benzene dimers. Larger basis set energy calculations and basis set superposition error calculations were performed for these benzene dimer configurations and are compared with the MP2/6-31G* calculations. For IPB, where dispersion effects are unlikely to be important in determining geometry, we performed SCF/6-31G*/MP2/6-31G* level calculations. Quantum chemistry calculations were performed using the quantum chemistry packages Gaussian94³⁵ and Mulliken³⁶ on IBM RS6000 workstations and a Cray C90 at NASA Ames.

Isopropylbenzene. The results of our SCF/6-31G*/MP2/6-31G* calculations of the conformational energy of IPB as a function of the torsional angle ψ are shown in Figure 3. Qualitatively our results are in agreement with previous studies.^{32,33} At the SCF level, the rotational energy barrier is 3.17 kcal/mol. The barrier decreases to 2.80 kcal/mol at the MP2 level. We have found that rotational energy barriers in hydrocarbons typically decrease when correlated methods are employed.³⁰

2,4-Diphenylpentane. The relative conformer energies for m-DPP and r-DPP are given in Table 1. Our SCF geometry optimizations and energy calculations (SCF/D95*) are in qualitative agreement with the STO-3G calculations of Lagowski et al.²⁴ For r-DPP, the r-*tt* and r-*gg* conformers are lowest in energy at this level because they involve no close (sterically

strained) interactions of either phenyl rings or the end methyl groups, as illustrated in Figure 2. All meso conformers contain sterically strained phenyl–phenyl, phenyl–methyl, and/or methyl–methyl interactions except m-*tg*, which at this level of theory is the lowest energy conformer. Quantitatively, it can be seen that the D95* basis set yields quite different relative conformer energies than were found at the STO-3G level.

The SCF/D95*/MP2/D95* energies differ qualitatively from the SCF values and demonstrate the influence of attractive dispersion effects between the phenyl rings on the relative conformer energies. This is best illustrated by the significant reduction in the relative energies of conformers containing eclipsed, sterically strained phenyl–phenyl configurations, specifically the r-*t \bar{g}* and the m-*tt* and m-*g \bar{g}* . When electron correlation is included in the geometry optimization, we can expect these conformers to become energetically even more favorable. We therefore performed MP2 geometry optimizations for the conformers found to be low energy at the SCF level (r-*tt*, r-*gg*, r-*tg*, m-*tg*) and for those likely to be strongly influenced by phenyl–phenyl dispersion interactions (r-*t \bar{g}* and m-*tt*). Unexpectedly, the relative energy for the m-*t \bar{g}* conformer dropped considerably at the SCF/D95*/MP2/D95* level compared to the SCF energy, so this conformer was also included in the MP2 geometry optimizations. (Geometry optimizations at the MP2/6-31G* level were performed for selected conformations because of the large computational requirements. This basis set yielded 295 basis functions for DPP. A geometry optimization for a typical conformer, beginning with SCF/D95* geometries, took approximately 500 h on an IBM RS6000 model 590.)

The 6-31G* SCF and MP2 energies at the MP2/6-31G* geometries are given in Table 1, while the MP2/6-31G* geometries are given in Table 2. Also given in Table 2 are the phenyl ring and backbone dihedral angles from the SCF/D95* geometries. The influence of electron correlation effects on geometries is illustrated in Figure 4 for the m-*tt* conformer. At the SCF level, the phenyl–phenyl interaction is unfavorable owing to steric and electrostatic interactions, and the molecular geometry is such as to relieve this interaction. At the MP2 level, attractive dispersion interactions result in a favorable phenyl–phenyl interaction, and the corresponding geometry yields a “parallel displaced-like” configuration of the phenyl rings similar to the lowest energy configuration of benzene dimer.³⁴ Computation of MP2 energies at the SCF geometries only partially accounts for the attractive phenyl–phenyl interactions because the SCF geometries do not reflect the influence of attractive phenyl–phenyl dispersion interactions on geometry. Unexpectedly, similar effects are seen for the r-*tt* and m-*t \bar{g}* conformers, where the phenyl rings are on opposite sides of the molecule backbone. For m-*t \bar{g}* , it can be seen in Figure 4 that, at the MP2 geometry, the phenyl rings are in closer proximity to each other, indicating more favorable phenyl–phenyl interactions than at the SCF level.

Phenyl–Phenyl Interactions. To better understand the nature of phenyl–phenyl interactions in the most important DPP conformers, and to investigate the accuracy of the MP/6-31G* level calculations in reproducing the interaction between phenyl rings, we employed the following procedure. The phenyl rings were extracted from the MP2/6-31G* geometries, and a hydrogen atom was added to fill the unsatisfied valence resulting from the broken C(sp²)–C(sp³) bond. The resulting benzene dimer geometries are shown in Figure 5 for representative conformers. It can be seen that when in close proximity, the phenyl rings prefer a parallel displaced-like arrangement that

TABLE 1: 2,4-Diphenylpentane Relative Conformer Energies from Quantum Chemistry Calculations

conformer	SCF/STO-3G ^a	SCF/D95*		MP2/6-31G*			
	SCF/STO-3G ^{b,c}	SCF/D95*	MP2/D95*	SCF/6-31G*	MP2/6-31G*	SCF/6-311G**	MP2/6-311G**
r- <i>tt</i>	0.00	0.00	0.00	0.00	0.00	0.00	0.00
r- <i>tg</i>	2.28	3.16	3.81	2.56	4.21		
r- <i>gg</i>	1.57	1.68	3.97	0.74	4.26	0.48	4.62
r- <i>ḡg</i>	4.73	5.43	5.99				
r- <i>t̄g</i>	4.29	6.02	4.03	8.24	2.47	8.24	1.24
r- <i>ḡḡ</i>	8.28	9.08	7.26				
absolute ^d	-647.542 164	-655.492 973	-657.610 292	-655.413 060	-657.624 696	-655.557 585	-657.976 470
m- <i>tt</i>	1.22	3.50	0.91	6.06	-1.05 (0.00) ^e	6.31	-2.40
m- <i>tg</i>	0.00	0.00	0.00	0.00	0.00 (1.05)	0.00	0.00
m- <i>gg</i>	2.67	2.96	3.87				
m- <i>ḡg</i>	3.71	4.39	3.29				
m- <i>t̄g</i>	2.77	3.33	1.44	4.06	0.73 (1.79)	4.23	0.23
m- <i>ḡḡ</i>	8.71	10.17	5.82				
absolute ^d	-647.540 994	-655.491 662	-657.606 990	-655.412 758	-657.620 933	-655.557 665	-657.972 380

^a The level of theory for geometries optimizations. ^b The level of theory for energy calculations. Energies in kcal/mol relative to the r-*tt* or the m-*tg* conformers. ^c From ref 24. ^d Absolute energies of the r-*tt* and m-*tg* conformers, in hartrees. ^e Relative to the m-*tt* conformer.

TABLE 2: 2,4-Diphenylpentane MP2 Geometries

	ϕ_1^a	ϕ_2	ψ_1^a	ψ_2	l_1^b	l_2	l_3	l_4	θ_1^c	θ_2	θ_3
r- <i>tt</i>	180.0 (173.2)	180.0 (173.2)	-59.9 (-60.1)	-59.9 (-60.1)	1.531	1.533	1.533	1.531	111.0	114.0	111.0
r- <i>gg</i>	60.9 (60.58)	60.89 (60.58)	-66.2 (-58.9)	-66.2 (-58.9)	1.531	1.537	1.537	1.531	112.3	115.5	112.3
r- <i>tg</i>	169.5 (162.3)	76.4 (76.1)	-60.8 (-58.9)	-63.2 (-61.1)	1.533	1.536	1.540	1.533	110.3	116.1	114.3
r- <i>t̄g</i>	179.8 (165.4)	-53 (-53.2)	-57.1 (-52.7)	-111.1 (-106.6)	1.533	1.535	1.544	1.526	109.9	117.1	111.9
m- <i>tt</i>	-179.4 (158.8)	-156.4 (158.2)	-59.5 (-59.4)	62.3 (59.7)	1.531	1.535	1.538	1.533	110.6	114.9	110.7
m- <i>tg</i>	-178.0 (176.6)	-63.59 (-65.3)	-58.7 (-58.9)	62.9 (65.1)	1.531	1.536	1.535	1.53	110.6	114.8	112.4
m- <i>t̄g</i>	171.5 (161.4)	78.3 (71.1)	-59.5 (-56.9)	104.8(98.9)	1.535	1.535	1.545	1.529	110.1	117.0	114.0

^a Backbone and phenyl ring torsional angles, racemic = *dl*, meso = *dd*. Numbers in parentheses are from SCF/D95* optimizations. ^b Backbone bond lengths, in Å. ^c Backbone valence angles, in deg.

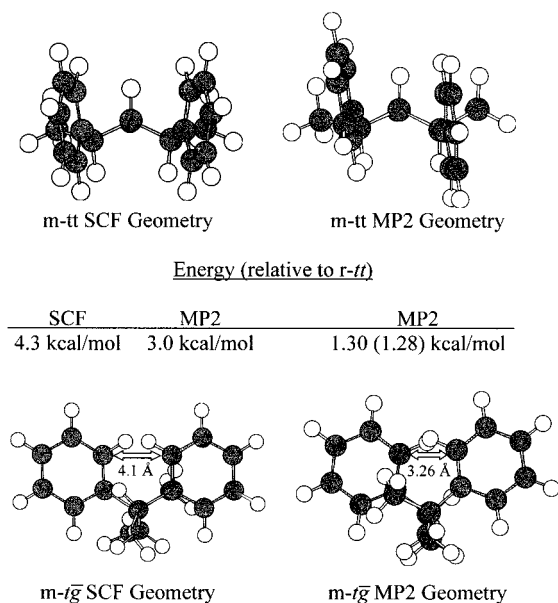


Figure 4. Comparison of SCF and MP2 geometries for selected 2,4-diphenylpentane conformers. SCF geometries were determined with a D95* basis set, and the corresponding SCF and MP2 energies were calculated with the same basis set. The MP2 geometry and corresponding energy was determined with a 6-31G* basis set. The number in parentheses is from MP2/D95*/MP2/D95* calculations.

corresponds to the lowest energy geometry of benzene dimer,³⁴ also illustrated in Figure 5. For the m-*tt* and r-*t̄g* conformers, where the phenyl rings are naturally eclipsed, the backbone distorts to allow a parallel displaced-like arrangement. This can be seen when comparing the SCF and MP2 geometries in Table 2. For the r-*tt* and the m-*tg* conformers, the phenyl rings are naturally parallel and the backbone distorts to allow *closer*

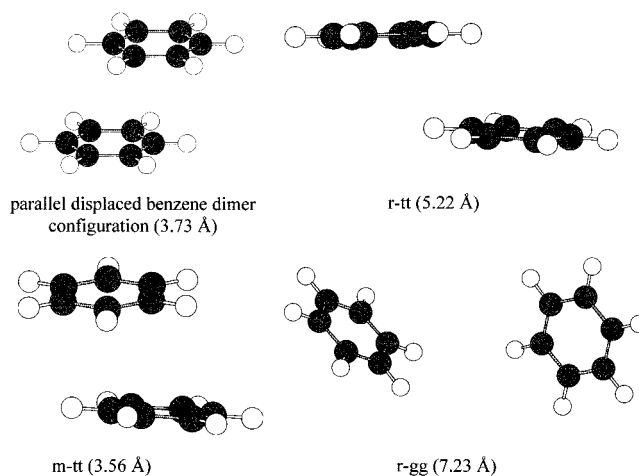


Figure 5. Benzene dimers corresponding to phenyl ring configurations extracted from MP2/6-31G* geometries of 2,4-diphenylpentane conformers. Numbers in parentheses indicate the center-of-mass separation.

contact between the phenyl rings. This accounts for the (unexpected) reduction of the energy of the m-*t̄g* conformer upon inclusion of electron correlation effects.

The binding energies for the extracted benzene dimer configurations were determined at the MP2/6-31G* and MP2/6-311G(2d,2p) levels with and without basis set superposition error (BSSE) correction using the counterpoise method. Our study of benzene dimer³⁴ demonstrated that the MP2/6-311G(2d,2p) energies with BSSE correction accurately represent the binding in this complex. A comparison of the energies is shown in Table 3. The agreement between the MP2/6-31G* energies without BSSE correction (the level of calculation used in our study of DPP) and the MP2/6-311G(2d,2p) energies with BSSE correction is reasonable.

TABLE 3: Phenyl–Phenyl Binding^a in Selected DPP Conformers

conformer	6-31G*				6-311G(2d,2p)				force field		
	SCF	MP2	BSSE(MP2)	MP2 (cor) ^b	SCF	MP2	BSSE(MP2)	MP2 (cor) ^b	LJ	electrostatic	total
r- <i>tt</i>	0.77	-2.31	1.88	-0.43	1.14	-3.44	1.54	-1.91	-1.78	-0.19	-1.98
r- <i>gg</i>	0.05	-0.29	0.08	-0.21	0.03	-0.44	0.13	-0.31	-0.36	0.04	-0.32
r- <i>tg</i>	-0.26	-0.75	0.28	-0.46	-0.30	-1.00	0.35	-0.64	-0.56	-0.01	-0.57
r- <i>t̄g</i>	7.64	-1.93	4.14	2.21	8.13	-5.48	3.49	-1.99	-2.66	0.52	-2.14
m- <i>tt</i>	7.76	-1.77	4.10	2.33	8.28	-5.29	3.45	-1.84	-2.75	0.93	-1.82
m- <i>tg</i>	-0.45	-1.16	0.44	-0.72	-0.47	-1.53	0.50	-1.03	-0.69	-0.05	-0.74
m- <i>t̄g</i>	0.39	-2.29	1.71	-0.58	0.71	-3.24	1.41	-1.83	-1.64	-0.47	-2.11

^a Relative to the benzene molecules at infinite separation, in kcal/mol. The MP2/6-31G* energies without BSSE correction and the MP2/6-311G(2d,2p) energies with BSSE correction are in bold. ^b With BSSE correction.

The difference between the SCF and MP2 energies emphasizes the importance of dispersion interactions between the phenyl rings. At the MP2 level, the interaction between phenyl rings is attractive for all configurations studied, while at the SCF level, it is attractive only for the m-*tg* and r-*tg* configurations, which have perpendicular phenyl ring orientations. The binding is greatest for the r-*tt* and m-*t̄g* configurations. However, the inclusion of electron correlation effects has the largest effect on the m-*tt* and r-*t̄g* conformers. This is because the dispersion effects are greatest for these configurations. Steric repulsion is also larger for the latter configurations, resulting in overall weaker binding. For all configurations the binding is significantly weaker than the -3.3 kcal/mol found for the parallel displaced benzene dimer.³⁴ Figure 5 reveals that for m-*tt* the phenyl rings are too close for optimal interactions, while for r-*tt* they are displaced too far “horizontally”.

Table 3 reveals that basis set superposition errors are large for the levels of theory employed. As discussed above, and demonstrated in Table 3, the MP2/6-31G* level calculations for benzene dimer yield reasonable binding energies *without* basis set superposition error correction when compared to the large basis set BSSE corrected values. When the MP2/6-31G* energies are corrected for BSSE, the binding is significantly underestimated because of inadequacies in the basis set. At the MP2/6-311G(2d,2p) level, the additional valence and polarization functions make up for many of the inadequacies in the smaller 6-31G* basis set, and the BSSE-corrected energies are in very good agreement with extrapolated values using larger basis sets and better electron correlation methods.³⁴ Without BSSE correction, the larger basis set seriously overestimates binding in benzene dimer. We suppose these trends hold also for DPP: we can obtain good conformer energies at the MP2/6-31G* level without BSSE correction, and better energies with larger basis sets (say MP2/6-311G(2d,2p)) *if we can correct for intramolecular BSSE*. Since this is not possible, until calculations can be performed with basis sets sufficiently large to make BSSE effects insignificant, we believe the MP2/6-31G* calculations are the most accurate that can be performed for obtaining relative conformer energies in DPP. The overestimation of phenyl–phenyl interactions that results from the use of larger basis sets is reflected in the 6-311G** energies given in Table 1.

Rotational Energy Barriers. We also determined the rotational energy barriers between important conformers of m-DPP and r-DPP. Specifically, we found the r-*tt*_t̄g, the m-*tt*_t̄g, and the m-*tt*_tg barriers in the following fashion. For the first two barriers, we performed a saddle point search at the SCF/6-31G* level to determine the torsional angle of the rotating dihedral. This torsion was then fixed, and an MP2/6-31G* optimization of the remaining degrees of freedom was performed. For the m-*tt*_tg barrier, the saddle point involves strong phenyl–phenyl interactions. Here, MP2 geometries were

TABLE 4: 2,4-Diphenylpentane Rotational Energy Barriers

conformer	energy (kcal/mol) ^a		dihedral angles			
	SCF	MP2	φ ₁	φ ₂	ψ ₁	ψ ₂
r- <i>tt</i> _t̄g	11.67	5.70	171.0	-114.1	-48.8	-83.9
m- <i>tt</i> _tg	-3.73	2.77	177.0	-100.0	-58.6	70.2
m- <i>tt</i> _t̄g	5.51	4.46	175.8	131.2	-47.9	100.5

^a MP2/6-31G* optimized geometry with fixed φ₂ (see text), using a 6-31G* basis set. Values are relative to the r-*tt* or m-*tt* conformers.

determined for several values of the torsional angle for the rotating dihedral in order to determine the saddle point geometry while including the effects of electron correlation for the rotating dihedral. The saddle point geometries and energies are summarized in Table 4. Figure 6 shows the conformational energy of m-DPP on the m-*tt*_tg path. The fit of

$$E(\phi_2) = 0.5 \left[\sum_{n=1}^3 k_n (1 - \cos n\phi_2) \right] \quad (1)$$

to the path indicates that the barrier is near φ₂ = -100°, the value reported in Table 4. The barriers are discussed below in conjunction with our molecular mechanics calculations.

III. Force Field Parametrization

An atomistic molecular mechanics force field was parametrized to reproduce the conformational energies and geometries of IPB and DPP given in Figure 3 and Tables 1, 2, and 4. The force field is given in Table 5. The nonbonded, stretch, bend, torsional, and out-of-plane deformation energies are given respectively by

$$E_{ij}^{\text{nb}} = E^{\text{lj}} + E^{\text{es}} = A_{ij} \exp(-B_{ij}r_{ij}) - C_{ij}/r_{ij}^6 + 332.08 q_i q_j / r_{ij} \quad (2)$$

$$E_{ij}^{\text{s}} = 0.5 k_s (r_{ij} - r_0) \quad (3)$$

$$E_{ijk}^{\text{b}} = 0.5 k_b (\theta_{ijk} - \theta_0)^2 \quad (4)$$

$$E_{ijkl}^{\text{t}} = 0.5 \left[\sum_{n=1}^3 k_n (1 - \cos n\phi_{ijkl}) \right] \quad (5)$$

$$E_{ijkl}^{\text{d}} = 0.5 k_d \theta_{ijkl}^2 \quad (6)$$

where r_{ij} , θ_{ijk} , ϕ_{ijkl} and θ_{ijkl} are the interatomic separation, valence angle, dihedral angle, and out-of-plane angle, respectively. The latter is given by the angle of bond jl with respect to the plane ijk .

The nonbonded dispersion/repulsion parameters for the aliphatic atoms (no subscript on the atom label in Table 5) have been used extensively by us in simulations of alkanes (e.g., refs

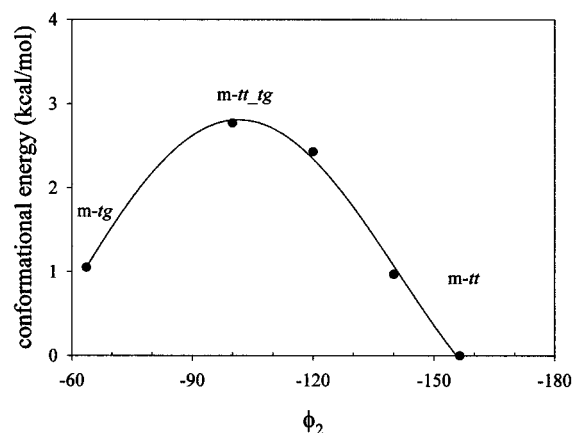


Figure 6. Conformational energy of m-DPP along the m-tt tg path. Energies are from MP2/6-31G*/MP2/6-31G* calculations. The solid line is a fit of eq 1 to the data.

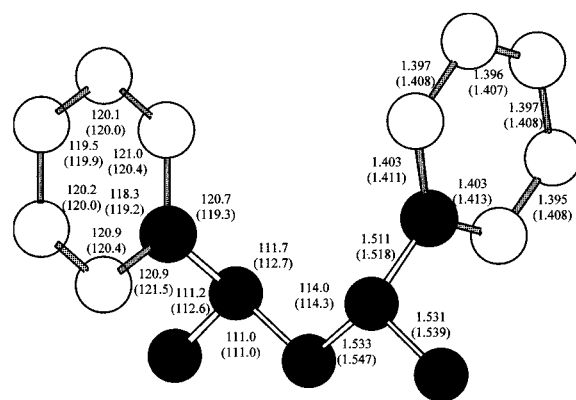


Figure 7. Valence geometry for the r-tt conformer of 2,4-diphenylpentane. Bond lengths (Å) and valence angles (deg) are from the MP2/6-31G* geometry. Force field values are given in parentheses. The white carbon atoms and attached hydrogen atoms are charged (see text).

37 and 38) and polyethers (e.g., refs 39 and 40). For the aromatic atoms (subscript "a"), the parameters were taken from our quantum chemistry based benzene force field.⁴¹ Aliphatic–aromatic cross terms were obtained using the geometric combining rule. The white aromatic carbon atoms ($q = -0.085$) and attached hydrogen atoms ($q = +0.085$) shown in Figure 7 are charged. This charge is a slight reduction from $q = \pm 0.11$ obtained in our study of benzene dimer.⁴¹ We found that we were able to obtain a better representation of the relative conformer energies in DPP with the reduced charge. All other atoms are charge neutral. The ability of the force field to reproduce the phenyl–phenyl nonbonded interactions is illustrated in Table 3. The molecular mechanics binding energies for the extracted benzene dimer configurations (taken for these calculations from the molecular mechanics DPP geometries) are in good agreement with quantum chemistry values.

The bond stretch and valence bending force constants were taken from the MOLBD3 force field.⁴² The equilibrium bond lengths and valence angles were adjusted to give the agreement between the molecular mechanics energy minimized and quantum chemistry (MP2/6-31G*) geometries of the r-tt conformer. As seen in Figure 7, agreement between the molecular mechanics and quantum chemistry geometries is good. The molecular mechanics bond lengths were parametrized to be about 0.01 Å larger than the quantum chemistry values to account for anharmonic effects. The parametrization of the torsional force constants for the C–C–C–C, the C–C–C–C_a and the C–C–C_a–C_a dihedrals is described below. The remaining

TABLE 5: Atomistic Force Field for 2,4-Diphenylpentane

nonbonded pair	A, kcal/mol	B, Å ⁻¹	C, kcal/mol Å ⁶
C–C	14969	3.09	640.5
C _a –C _a	78998	3.6	519.0
H–H	2684	3.73	27.3
H _a –H _a	2384	3.74	24.62
C _a –H _a	3888.	3.415	124.4
C–H	4318.	3.415	138.2
C–H _a , C _a –H	4097.	3.415	131.1
H–H _a	2530	3.74	26.0
C–C _a	34388	3.335	576.6

stretch	k_s , kcal/mol Å ²	r_0 , Å
C–C	618	1.53
C _a –C _a	1102	1.40
C–C _a	634	1.50
C–H	655	1.09
C _a –H _a	727	1.09

bend	k_b , kcal/mol rad ²	Θ_0
C–C–H	86.1	109.5
C–C–C	108.1	111.0
C–C–C _a	108.1	110.4
C–C _a –C _a	100.8	120.0
H–C(methyl)–H	77.1	107.9
H–C–H	77.1	106.5
C _a –C–H _a	72.0	120.0
C–C–C _a	108.1	108.9
C _a –C _a –C _a	144.0	120.0

torsion	k_1 , kcal/mol	k_2 , kcal/mol	k_3 , kcal/mol
C–C–C–C	1.82	1.96	−0.04
C–C–C–C _a	1.64	0.58	−0.04
C–C–C–H	0.00	0.00	−0.23
C–C–C _a –C _a	0.00	0.32	0.00
C–C _a –C _a –C _a	0.00	0.00	0.00
C–C _a –C _a –H _a	0.00	0.00	0.00
H–C–C–H	0.00	0.00	−0.23
C _a –C–C–H	0.00	0.00	−0.23
C _a –C _a –C–H	0.00	0.00	0.00
C _a –C _a –C _a –H _a	0.00	0.00	0.00
C _a –C _a –C _a –C _a	0.00	25.00	0.00
H _a –C _a –C _a –H _a	0.00	0.00	0.00
H–C–C–H	0.00	0.00	−0.23

out-of-plane deformation	k_d , kcal/mol rad ²
C–C _a –C _a –C _a	0.00
H _a –C _a –C _a –C _a	0.00
C _a –C _a –C _a –H _a	41.8
C _a –C _a –C _a –C	41.8

torsional parameters and all of the out-of-plane deformation force constants were taken from previous work.^{26,41} The energy required to displace a hydrogen atom out of the plane of a phenyl ring (maintaining C_s symmetry) was examined at the 6-31G* MP2 level and was found to be in good agreement with molecular mechanics predictions.⁴³

Phenyl Ring Rotation. The only undetermined parameters influencing the energetics for rotation of the phenyl ring in IPB are the force constants for the C–C–C_a–C_a torsional potential. As can be seen in Figure 3, an excellent representation of the quantum chemistry energies is obtained with $k_2 = 0.32$ kcal/mol.

Backbone Dihedrals. Having established the parameters for valence and nonbonded interactions as well as the phenyl ring rotation, the conformational energetics in DPP are determined by the torsional parameters for the C–C–C–C, the C–C–C–C_a dihedrals. A nonlinear least-squares fitting procedure was employed to obtain the best fit to the ab initio conformer energies and rotational energy barriers. Comparison of the MP2/6-31G* phenyl–phenyl interaction energies with the MP2/

TABLE 6: 2,4-Diphenylpentane Conformer and Barrier Energies

conformer	energy (kcal/mol) ^{a,b}	
	force field	MP2/6-31G*
r- <i>tt</i>	0.00	0.00
r- <i>t</i> \bar{g}	2.17	2.47 (2.07) ^c
r- <i>gg</i>	3.79	4.26 (3.86)
r- <i>tg</i>	3.50	4.21 (3.81)
r- <i>g</i> \bar{g}	6.15	
r- <i>g</i> \bar{g}	6.17	
r- <i>tt</i> _ <i>t</i> \bar{g}	5.46	5.70 (5.30)
m- <i>tt</i>	0.00	0.00
m- <i>tg</i>	1.09	1.05
m- <i>t</i> \bar{g}	1.99	1.79 (2.19)
m- <i>gg</i>	4.96	
m- <i>g</i> \bar{g}	4.14	
m- <i>g</i> \bar{g}	5.57	
m- <i>tt</i> _ <i>tg</i>	2.65	2.78
m- <i>tt</i> _ <i>t</i> \bar{g}	4.20	4.46

^a Relative to the rr-*tt* or m-*tt* conformers. Quantum chemistry values are from MP2/6-31G*/MP2/6-31G* calculations (see text for discussion of barrier calculations). ^b Force field was parametrized to reproduce boldfaced energies. ^c Energies in parentheses are corrected for estimated errors in phenyl-phenyl interaction energies (see text).

TABLE 7: 2,4-Diphenylpentane Conformer Geometries from Force Field Calculations

	ϕ_1^a	ϕ_2	ψ_1^a	ψ_2
r- <i>tt</i>	-178.4	-178.4	-56.9	-56.9
r- <i>gg</i>	54.7	54.7	-65.9	-65.9
r- <i>t</i> \bar{g}	175.5	-47.3	-55.5	-109.2
r- <i>tg</i>	166.0	61.1	-53.3	-66.3
r- <i>g</i> \bar{g}	60.7	-88.7	-67.1	-112.4
r- <i>g</i> \bar{g}	-74.9	-74.9	-110.0	-110.0
m- <i>tt</i>	167.5	-166.8	-59.08	59.09
m- <i>tg</i>	-177.4	-55.7	-54.0	66.5
m- <i>t</i> \bar{g}	171.3	77.7	-56.4	104.0
m- <i>gg</i>	54.6	-94.7	-66.9	55.7
m- <i>g</i> \bar{g}	58.0	51.3	-67.0	117.8
m- <i>g</i> \bar{g}	-82.8	-49.4	-113.5	111.6

^a Backbone and phenyl ring torsional angles, racemic = *dl*, meso = *dd*.

6-311G(2d,2p) BSSE-corrected values indicates that the former level calculations tend to overestimate this interaction by about 0.4 kcal/mol in the r-*tt* and m-*t* \bar{g} conformers. Therefore, the energies for these conformers were increased by 0.4 kcal/mol, yielding the modified MP2/6-31G* values shown in Table 6. The molecular mechanics energies given in Table 6 are in good agreement with these values. Table 7 reveals that the force field also does an excellent job in reproducing the quantum chemistry geometries for the important DPP conformers (compare with Table 2). As a consistency check, the energy difference between the r-*tt* and m-*tt* conformers yielded by the force field is $\Delta = 1.01$ kcal/mol, in good agreement with the (modified) MP2/6-31G* value of $\Delta = [1.30$ (from q.c.) $- 0.4$ (increase in r-*tt* energy discussed above)] = 0.90 kcal/mol. This energy difference was not considered in the force field parametrization.

IV. 2,4-Diphenylpentane Conformational Energy Surfaces

Figures 8 and 9 are energy contour maps showing the conformational energies of r-DPP and m-DPP as a function of the backbone dihedral angles, determined from molecular mechanics calculations using the quantum chemistry based force field. The backbone dihedral angles were fixed at 10° intervals, and the geometry was optimized with respect to the remaining

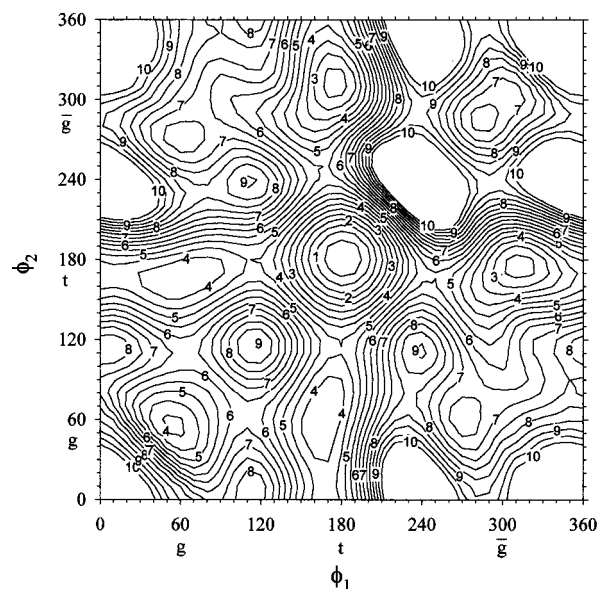


Figure 8. Conformational energy contour map for racemic 2,4-diphenylpentane obtained from the quantum chemistry based force field. Energies are in kcal/mol relative to the r-*tt* conformer.

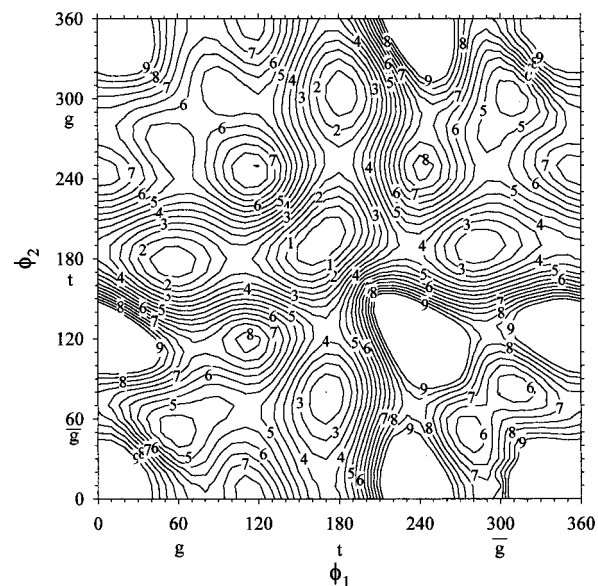


Figure 9. Conformational energy contour map for meso-2,4-diphenylpentane obtained from the quantum chemistry based force field. Energies are in kcal/mol relative to the m-*tt* conformer.

degrees of freedom. The only unexpected feature of the energy surface revealed by the contour maps is the split minimum for the m-*gg* and m-*g* \bar{g} conformers. These conformers are unimportant for the isolated molecules but may be important in condensed phases.

The contour plots reveal that the m-*tt*_*tg* barrier is unique in that it is the only rotational energy barrier lower than 3 kcal/mol for either enantiomer. The low-energy path between the m-*gt* and m-*tg* conformers, thought to be the most important meso conformers in solution, involves *tt*_*tg* (*gt* \leftrightarrow *tt* \leftrightarrow *tg*) transitions. The contour plots reveal that the only low-energy rotational isomerization path (<6 kcal/mol) we failed to investigate at the MP2/6-31G* level involves the r-*tt*_*tg* barrier, which the force field predicts to be around 4.5 kcal/mol. The *tg* conformer is too high in energy to have an appreciable population (at least for isolated molecules). Condensed-phase experiments, however, have been interpreted in terms of an

TABLE 8: DPP Conformer Populations

conformer	molecular mechanics 450 K		gas-phase (MD) 450 K	
	racemic	meso	racemic	meso
<i>tt</i>	0.810 (0.00) ^a	0.546 (0.00)	0.770 (0.00)	0.282 (0.00)
<i>tg</i> or <i>gt</i>	0.016 (3.50)	0.161 (1.09)	0.049 (2.75)	0.313 (−0.09)
<i>t̄g</i> or <i>ḡt</i>	0.071 (2.17)	0.059 (1.99)	0.029 (3.26)	0.033 (1.91)
<i>gg</i>	0.014 (3.79)	0.002 (4.96)	0.052 (2.69)	0.012 (2.78)
<i>ḡg</i> or <i>ḡḡ</i>	<0.001 (6.15)	0.005 (4.14)	0.006 (4.87)	0.006 (3.43)
<i>ḡḡ</i>	<0.001 (6.17)	0.001 (5.57)	<0.001 (7.47)	<0.001 (6.04)

^a Numbers in parentheses are relative free energies in kcal/mol.

appreciable *r-gg* population in addition to *r-tt*. For the isolated molecule, the low energy *r-tt_gg* path involves *tt_tg* transitions.

V. Gas-Phase Simulations

The racemic and meso conformer populations determined from molecular mechanics calculations are given in Table 8 at 450 K, assuming that the statistical weight of each conformer can be represented as a Boltzmann factor employing the molecular mechanics energies given in Table 6. For isolated molecules *r*-DPP is largely *r-tt* and *m*-DPP is a mixture of *m-tt* and *m-tg*, with the former being the most important. These populations are inconsistent with those obtained from interpretations of condensed-phase experiments. In the condensed phases, conformer populations are likely to be quite different from those yielded by the relative conformer energies. The latter populations do not take into account differences in the shape of the energy surface for each conformer nor account for the ability of conformers such as *m-tg* to more effectively interact with solvent molecules than conformers such as *m-tt*, as illustrated in Figure 1. This latter effect will be considered in an upcoming paper where we will report on molecular dynamics simulations of liquid-phase DPP employing our quantum chemistry based force field.

We have investigated the effect of the shape of the energy surface on conformer populations (independent of intermolecular interactions) by performing gas-phase molecular dynamics simulations. Simulations were performed on an ensemble of 100 (noninteracting) *m*-DPP molecules and on an ensemble of 100 *r*-DPP molecules at 298, 450, and 500 K using the stochastic dynamics algorithm described elsewhere.⁴⁴ Bond lengths were constrained, while all other degrees of freedom remained flexible. Using a time step of 1 fs, 1 ns equilibration and 300 ps sampling runs were performed. After several hundred picoseconds of equilibration time, the conformer populations stabilized, indicating that the gas-phase systems had equilibrated. We believe that longer equilibration times may be necessary in the condensed phases, where conformational dynamics will be much slower. The resulting conformer populations at 450 K are given in Table 8. These populations differ significantly from those given by the relative conformer energies. The relative (to *tt*) free energy of a conformer *i* can be computed from the relationship

$$\Delta A_i = RT \ln p_{tt}/p_i \quad (7)$$

where p_i is the population of conformer *i*. The relative free energies are given in Table 8 at 450 K. From the molecular mechanics populations, the relative free energies are the same as the relative conformer energies in Table 6 and are temperature-independent. From the gas-phase populations, the relative free energies are significantly different from the relative conformer energies and are quite temperature-dependent. From the relative free energies obtained at 298, 450, and 500 K, the

relative energies and entropies of the conformers were determined from the relationship

$$\Delta A_i = \Delta E_i - T\Delta S_i \quad (8)$$

which was found to represent ΔA_i quite well. Here it is assumed that ΔE_i and ΔS_i are independent of temperature. The relative energies were found to be nearly identical to the relative conformer energies in Table 6. The relative entropies are given in Figure 2. For both enantiomers, conformers with phenyl rings aligned at the ends of the molecule and parallel to the molecular backbone (such as *m-gg*) have the greatest entropy. This alignment allows the maximum rotational freedom for the phenyl rings. Form *m*-DPP, the next highest entropy configuration, involves a phenyl ring perpendicular to the chain backbone. The same alignment, but eclipsing a methyl group, has lower entropy. Finally, conformers with eclipsed phenyl rings, such as *m-tt*, have the lowest entropy. Note that energetically, this conformer results in favorable phenyl–phenyl interactions, as discussed above, but the consequent restrictions on phenyl rotation results in a large entropy penalty. Similar trends can be seen for *r*-DPP. The entropic effects are important: Table 8 reveals that while energetically the *m-tt* conformer is more than 1 kcal/mol lower in energy than the *m-tg*, the latter has a greater population in the gas phase at 450 K.

Acknowledgment. G.D.S. acknowledges support of NASA Grant NAG 1 1984 and ACS-PRF Grant 30333-G7 for this work.

References and Notes

- (1) Mondello, M.; Yang, H. J.; Furuya, H.; Roe, R. J. *Macromolecules* **1994**, *27*, 3566.
- (2) Furuya, H.; Mondello, M.; Yang, H. J.; Roe, R. J.; Erwin, R. W.; Han, C. C.; Smith, S. D. *Macromolecules* **1994**, *27*, 5674.
- (3) Roe, R. J.; Mondello, M.; Furuya, H.; Yang, H. J. *Macromolecules* **1995**, *28*, 2807.
- (4) Han, J.; Gee, R. H.; Boyd, R. H. *Macromolecules* **1994**, *27*, 7781.
- (5) Han, J.; Boyd, R. H. *Polymer* **1996**, *37*, 1797.
- (6) Rapold, R. F.; Suter, U. W.; Theodorou, D. N. *Macromol. Theory Simul.* **1994**, *3*, 19.
- (7) Khare, R.; Paulaitis, M. E.; Lustig, S. R. *Macromolecules* **1993**, *26*, 7203.
- (8) Khare, R.; Paulaitis, M. E. *Macromolecules* **1995**, *28*, 4495.
- (9) Zoidis, E.; Borsdorf, Ch.; Strehle, F.; Dorfmueller, Th. *Chem. Phys.* **1992**, *168*, 99.
- (10) Bovey, F. A.; Hood, F. P., III; Anderson, E. W.; Snyder, L. C. J. *Chem. Phys.* **1965**, *42*, 3900.
- (11) Doskocilova, D.; Schneider, B. J. *Polym. Sci. B* **1965**, *3*, 213.
- (12) Bovey, F. A. *High-Resolution NMR of Macromolecules*; Academic Press, New York, 1971; 190 and references contained therein.
- (13) Pivcova, H.; Kolinsky, M.; Lim, D.; Schneider, B. J. *Polym. Sci. C* **1969**, *22*, 1093.
- (14) Fourche, G.; Lemaire, B. *Polym. J.* **1973**, *4*, 476.
- (15) Fourche, G.; Jasse, B.; Maelstaf, P. *Polym. J.* **1977**, *9*, 537.
- (16) Jasse, B.; Monnerie, L. *J. Phys. D: Appl. Phys.* **1975**, *8*, 863.
- (17) Froelich, B.; Noel, C.; Jasse, B.; Monnerie, L. *Chem. Phys. Lett.* **1976**, *44*, 159.
- (18) Froelich, B.; Jasse, B.; Noel, C.; Monnerie, L. *Faraday Trans. 2* **1978**, *74*, 445.
- (19) Williams, A. D.; Brauman, J. I.; Nelson, N. J.; Flory, P. J. *J. Am. Chem. Soc.* **1967**, *89*, 4807.
- (20) Williams, A. D.; Flory, P. J. *J. Am. Chem. Soc.* **1969**, *91*, 3111.
- (21) Yoon, D. Y.; Sundararajan, P. R.; Flory, P. J. *Macromolecules* **1975**, *8*, 776.
- (22) Stegen, G. E.; Boyd, R. H. *Polym. Prepr.* **1978**, *19*, 595.
- (23) Rapold, R. F.; Suter, U. W. *Macromol. Theory Simul.* **1994**, *3*, 1.
- (24) Lagowski, J. B.; Vancso, G. J. *Int. J. Quantum Chem.* **1993**, *46*, 271.
- (25) Smith, G. D.; Jaffe, R. L. *J. Phys. Chem.* **1996**, *100*, 18718.
- (26) Smith, G. D.; Yoon, D. Y. *J. Chem. Phys.* **1994**, *100*, 649.
- (27) Smith, G. D.; Jaffe, R. L.; Yoon, D. Y. *Macromolecules* **1994**, *27*, 3166.

- (28) Smith, G. D.; Ludovice, P. J.; Jaffe, R. L.; Yoon, D. Y. *J. Phys. Chem.* **1995**, *99*, 164.
- (29) Smith, G. D.; Jaffe, R. L.; Yoon, D. Y. *J. Phys. Chem.* **1993**, *97*, 12752.
- (30) Smith, G. D.; Paul, W. *J. Phys. Chem.* in press.
- (31) Jaffe, R. L.; Smith, G. D.; Yoon, D. Y. *J. Mol. Struct.*, submitted.
- (32) Schaefer, T.; Sebastian, R.; Penner, G. H. *Can. J. Chem.* **1988**, *66*, 1495.
- (33) Lagowski, J. B.; Csizmadia, I. C.; Vancso, G. J. *J. Mol. Struct.: THEOCHEM* **1992**, *258*, 341.
- (34) Jaffe, R. L.; Smith, G. D. *J. Chem. Phys.* **1996**, *105*, 2780.
- (35) Frisch, M. J.; Trucks, G. W.; Schlegel, H. B.; Gill, P. M. W.; Johnson, B. G.; Robb, M. A.; Cheeseman, J. R.; Keith, T.; Petersson, G. A.; Montgomery, J. A.; Raghavachari, K.; Al-Laham, M. A.; Zakrzewski, V. G.; Ortiz, J. V.; Foresman, J. B.; Cioslowski, J.; Stefanov, B. B.; Nanayakkara, A.; Challacombe, M.; Peng, C. Y.; Ayala, P. Y.; Chen, W.; Wong, M. W.; Andres, J. L.; Replogle, E. S.; Gomperts, R.; Martin, R. L.; Fox, D. J.; Binkley, J. S.; Defrees, D. J.; Baker, J.; Stewart, J. P.; Head-Gordon, M.; Gonzalez, C.; Pople, J. A. *Gaussian 94*, Revision D.1; Gaussian, Inc.: Pittsburgh, PA, 1995.
- (36) Mulliken 2.0 is a quantum chemistry code developed by IBM Research Division, Chemical Services and Applications, Almaden Research Center, 1995.
- (37) Smith, G. D.; Yoon, D. Y.; Jaffe, R. L. *Macromolecules* **1995**, *28*, 5897.
- (38) Smith, G. D.; Paul, W.; Yoon, D. Y.; Zirkel, A.; Hendricks, J.; Richter, D.; Schober, H. *J. Chem. Phys.* **1997**, *107*, 4751.
- (39) Smith, G. D.; Yoon, D. Y.; Jaffe, R. L.; Colby, R. H.; Krishnamoorti, R.; Fetters, L. J. *Macromolecules* **1996**, *29*, 3462.
- (40) Smith, G. D.; Yoon, D. Y.; Wade, C. G.; O'Leary, D.; Chen, A.; Jaffe, R. L. *J. Chem. Phys.* **1997**, *106*, 3798.
- (41) Smith, G. D.; Jaffe, R. L. *J. Phys. Chem.* **1996**, *100*, 9624.
- (42) Boyd, R. H.; Breitling, S. M.; Mansfield, M. L. *AIChE J.* **1973**, *19*, 1016.
- (43) Best agreement was found when the $C_a-C_a-C_a-H_a$ force constant was reduced slightly from 41.8 as given in Table 5 to 38.6.
- (44) Smith, G. D.; Jaffe, R. L.; Yoon, D. Y. *Macromolecules* **1993**, *26*, 298.